

Synthesis of nanosized SnO/ZnO coupled oxides via co-precipitation method

M. R. Vaezi*

Division of Nanotechnology and Advanced Materials, Materials and Energy Research Center, Karaj, Iran

In this paper, SnO/ZnO nanocomposites have been produced via co-precipitation method for the first time. SnCl₂, ZnCl₂ and NaOH were used as precursors. The synthesized powders were characterized by X-Ray Diffraction (XRD), scanning electron microscope (SEM), transmission electron microscope (TEM), Brunauer-Emmett-Teller adsorption isotherm (BET) and X-ray fluorescence (XRF) analyses. Effect of synthesis temperature on the obtained phases, particle size and morphology, crystallite size and specific surface area of produced nanocomposites have been discussed. It has been shown that at lower synthesis temperature only ZnO nanocrystals could be produced, however at higher temperatures SnO/ZnO nanocomposites could be formed and this co-existence of phases affects the powders crystallite sizes, morphologies, particle sizes and specific surface areas.

Key words: Coupled oxide, SnO, ZnO, Co-precipitation, Nanocomposites.

Introduction

Semiconductor oxide materials (e.g. SnO₂, ZnO, TiO₂, ZrO₂, WO₃, etc) have been attracted scientists' interests recently because of their wide applications in photocatalysts, gas sensors, liquid crystal displays, photovoltaic cells, transparent electrodes and lasers, etc [1]. Also, coupling of two semiconductor nano oxide has been studied in the past few years. It has been shown that by using two semiconductor nano oxides together the properties of these oxides would change [1-7].

Wang Cun et al reported the synthesis of ZnO/SnO₂ coupled oxides [8]. They compared the photocatalytic activity of ZnO/SnO₂ nano composites with their separate oxides. They observed that the photocatalytic activity of ZnO/SnO₂ nano composite was much more than SnO₂ and ZnO separately. They also proposed that its higher activity is because of lower recombination rate of electron-hole pairs in composite form. Similar results have been reported in literature [4, 9-10]. Additionally Jinghong Li et al showed that by coupling nano oxides they usually show higher crystallinity and thermal stability, which can enhance their performance [10].

Coupled oxides have been produced by several methods, such as: hydrothermal [11], chemical bath deposition [2], chemical vapor deposition [12], sol-gel [13, 14] and solid state techniques [15, 16]. Among the chemical methods that have been reported in literature,

the most common way for production of these nano size coupled oxides is co-precipitation method [4, 8].

Recently, methods for obtaining nano- sized coupled SnO₂/ZnO are intensively developed and studies have been focused on production and characterization of these coupled oxides [4, 6, 9, 17, 18].

A continual challenge for the researchers is to fabricate metal oxide materials, by controlling the oxidation state of multi valence metals ions in solutions. Although some studies have been conducted for production of nanosized SnO₂/ZnO coupled oxides, but the control of oxidation state of tin oxide in an aqueous solution in these coupled oxides has hardly been investigated.

Due to the fact that Sn(II) is easily oxidized to Sn(IV), production of SnO/ZnO coupled nano oxide is relatively difficult. Thus, very few articles have been reported on the synthesizing of tin monoxide (SnO) [19-25] and to authors' best knowledge, no article on the synthesis of SnO/ZnO nanosized coupled oxide has been published till date.

In the present paper for the first time, fabrication of SnO/ZnO nanosized coupled oxide with oxidation state of II for tin in solution by using the simple method of co-precipitation is reported. These nanosized coupled oxides were obtained using SnCl₂ · H₂O and ZnCl₂ as precursors at three different temperatures. Due to the high specific surface area of the obtained powders, these nanosized coupled oxides have very good potential for applications in gas sensors, photo-catalysis and photo-electrochemical cells.

Experimental

All of the chemical reagents which used in the

*Corresponding author:
Tel : +98-26-36204131
Fax: +98-21-88773352
E-mail: m_r_vaezi@merc.ac.ir

experiments were analytical grade and used without further purification and treatment. The procedure employed for preparing SnO/ZnO nano composites was as following: Two aqueous solutions of SnCl₂ and ZnCl₂ (1M, 100 ml) were added simultaneously dropwise to an aqueous solution of NaOH (4M, 100 ml) within about 30 min under vigorous stirring condition. This process was carried out at different temperatures of 25 °C (sample I), 50 °C (sample II) and 75 °C (sample III) in beakers, each placed in a thermostatic cooling-heating water bath. Then the samples were kept for additional 2 hours under the same stirring condition and temperature. After synthesis, the powders were centrifuged and washed several times with distilled water and absolute ethanol and tested for removing of impurities specially NaCl with AgNO₃ and dried at 50 °C in an oven. The obtained powders characterized by X-Ray diffraction, SEM, TEM, XRF and BET techniques.

Results and Discussion

The obtained phases are listed in Table 1. As shown in Table 1, final color of the synthesized sample at room temperature was pale yellow and the rest were dark green while becoming darker by increase in temperature. During the synthesis of the sample I (at room temperature) the solution was always pale yellow, but for the other solutions after addition of certain amount of metal chloride solution that causes decrease in solutions pHs, the color of samples changed suddenly to dark green. It was observed that for sample III, this change in color occurred sooner than sample II.

Table 1. Synthesized powders.

sample	Synthesized temperature (°C)	Color	Obtained phases
I	25	Pale yellow	ZnO
II	50	Dark Green	SnO, ZnO
III	75	Dark Green	SnO, ZnO

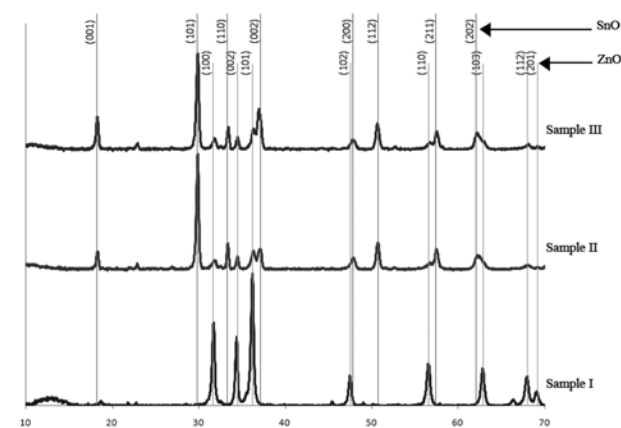


Fig. 1. X-Ray diffraction patterns of powders synthesized at 25 °C (sample I), 50 °C (sample II), and 75 °C (sample III).

Also, by increasing the temperature from 25 °C to 50 °C the amount of the obtained powder increased drastically, as their initial solutions were the same.

X-Ray diffraction patterns of the samples are shown in Fig.1. Brags peaks in sample I showed good agreement with ZnO (JCPDS no.36-1451), and no brag peaks of other compounds were found. But for the sample II and III the peaks are related to SnO (JCPDS no.06-0395) as well as ZnO (JCPDS no.36-1451).

Also, XRF analysis of sample I (Table 2) indicated existence of about 85.3 percent ZnO and 10.2 percent of SnO in the sample. Sn atoms can be doped in ZnO structure as two precursors of Zn and Sn are mixed together. As cited above, due to lack of SnO peaks in the XRD pattern of sample I, Sn should be formed as amorphous SnO or doped in ZnO during synthesis process. In fact this amount of doped Sn in comparison with the amount of Sn for Sample I is little enough to conclude that the major amount of Sn atoms have to be formed as individual amorphous phase instead of dopant in ZnO. J. Chouvin et al. reported synthesizing of SnO nano particles via CBD method. They used aqueous solutions of SnCl₂.2H₂O and NaOH as precursors of SnO and reported that by increasing temperature up to the boiling point, the mixtures' color turned from white to black and SnO crystals were formed during nucleation and growth of the previous amorphous phase [26]. This fact can be observed in

Table 2. Results of XRF analysis of samples.

Sample	Percentage of Products (%Wt)		
	ZnO	SnO	Other Products
I	85.3	10.2	4.5
II	48.2	48.6	3.2
III	51.7	45.6	2.7

Table 3. Mean crystallite sizes and lattice constants of prepared samples.

Sample	ZnO		SnO	
	Crystallite size (nm)	c/a	Crystallite size (nm)	c/a
I	23.56	1.600	---	---
II	14.97	1.599	23.95	1.280
III	15.34	1.598	24.90	1.284

Table 4. Specific surface area from BET, Mean aggregates size from SEM and mean particle size from TEM.

Sample	BET surface area (m ² g ⁻¹)	Mean aggregates size (nm)	Mean particle size (nm)
I	16.28	58 in width 260 in diagonal	45.2
II	22.88	58.4	34.4
III	19.84	52.4	36.5

this synthesis process too. The variation of obtained phase's ratio with increasing of synthesis temperature can be correlated to this phenomenon.

The average crystallite size is calculated from the full width at half maximum (FWHM) of the diffraction peaks using the Debye-Scherer formula:

$$D = k\lambda/\beta\cos\theta \quad (1)$$

where D is the mean crystallite size; K is a grain shape dependent constant (here assumed to be 0.89); λ is the wavelength of the incident beam; θ is the Bragg reflection peak; and β is the full width at half maximum [27]. As can be seen in Table 3, the mean crystallite size of SnO particles from their (101) planes are 23.95 and 24.90 for 50 and 75 °C, respectively. It can be seen from (002) plane of ZnO XRD patterns, at 25 °C the mean crystal size of ZnO is about 23.56 nm but by increase in temperature to 50 and 75 °C it decreased to 14.97 and 15.34 nm respectively. This decrease can be concluded from changing of obtained morphologies and growth conditions while increasing temperature [28, 29]. The results are listed in Table 3. Moreover the XRD results, at room temperature SnO wouldn't be formed, so the final pH of this solution would be higher because of higher hydroxyl groups that remained in the solution. As existence of higher hydroxyl groups favors the growth of the crystalline phases; this condition favors the faster growth of ZnO crystals. As a result their crystallite sizes would be higher. Also it has been reported in literature that in this method, co-existence of seconds phase hinders the growth of crystals [7].

SEM images of samples are shown in Fig. 2. For particles of sample I, at the first glimpse it may look like that they are disc like particles but more precise investigation reveals that they are agglomerations of many tiny particles with 456.2 nm mean particle size.

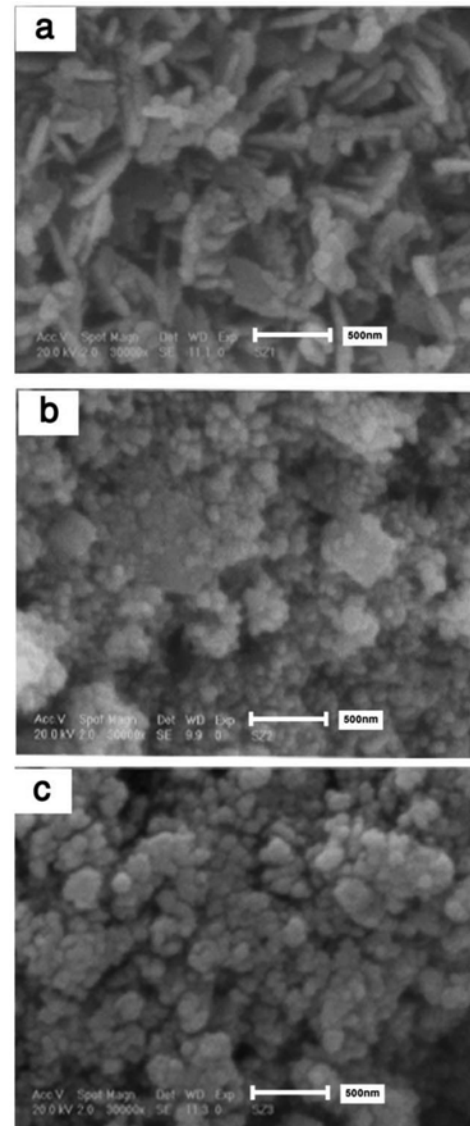


Fig. 2. SEM images of obtained powders at (a) 25, (b) 50 and (c) 75 °C.

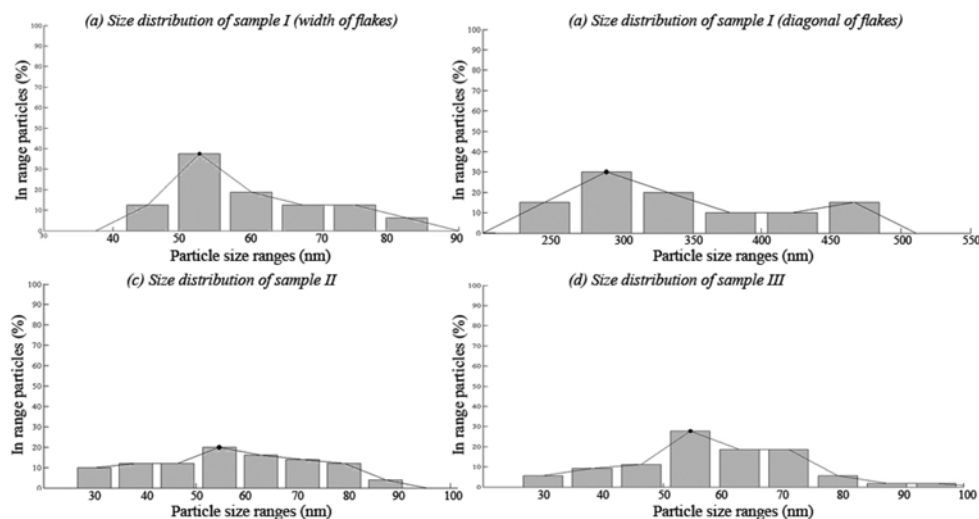


Fig. 3. Agglomerates size distribution of samples: (a) I (flakes width), (b) I (flakes diagonals), (c) II and (d) III.

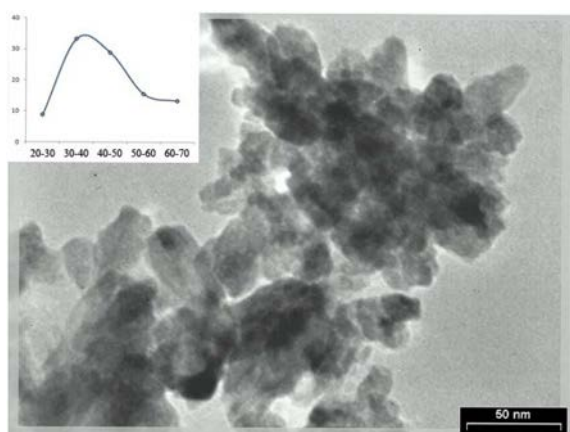


Fig. 4. TEM image of sample II with measured size distribution.

Mean particles sizes of samples are measured and listed in Table 4. Also, agglomerates size distribution of samples is shown in Fig. 3.

It was found that at 25 °C, ZnO particles produce flake like agglomerates with median size of about 58 nm in width and 260 nm in diagonal as shown in Fig. 2a, but in fact this agglomerates are formed by smaller particles. At 50 °C and 75 °C the median sizes of obtained semispherical agglomerates of ZnO/SnO coupled oxides were 58.4 nm and 52.4 nm, respectively. From TEM images, these agglomerates as shown in Fig. 4, are formed from individual nanoparticles. The median sizes of obtained nanoparticles from TEM images and the agglomerates median sizes are listed in Table 4. As it can be seen, by change in temperature the sizes of obtained powders haven't changed intensively from sample II to III. But as listed in Table 4, due to enhancement in agglomeration, the specific surface area of the obtained samples are decreased by increasing synthesis temperature from 50 to 75 °C.

The specific surface area of the obtained samples was calculated from Brunauer-Emmett-Teller (BET) equation and listed in Table 4. As it can be seen, BET surface area of obtained powders are 16.28, 22.88, 19.84 m²g⁻¹ for synthesized powders at 25, 50 and 75 °C, respectively. The lower surface area of sample I should be attributed to intense agglomeration of the particles in the form of plates. As mentioned above higher surface area of sample II is because of its lower agglomeration and also lower particle size.

Conclusions

In this article, synthesis of coupled SnO/ZnO nanoparticles via simple and cost-effective method of co-precipitation is reported. The powders are synthesized at different temperatures and their properties were studied by using different techniques. Results showed that SnO/ZnO coupled oxide produced at higher temperature with lower crystalline size and higher specific surface areas.

References

1. J.A. Rodríguez and M.F. García, Synthesis, properties, and applications of oxide nanomaterials, Wiley, New York, 2007.
2. V.P. Tai., J.H. Oh, Sensor. Actuat. B. 85 (2002) 154.
3. A. Erkan, U. Bakir and G. Karakas, J. Photoch. Photobio. A. 184 (2006) 313.
4. M. Zhang, T. An, X. Hu, C. Wang, G. Sheng and J. Fu, Appl. Catal. A-Gen. 260 (2004) 215.
5. J.L. Solis and V. Lantto, Sensor. Actuat. B-Chem. 48 (1998) 322.
6. B.P.J. de Lacy Costello, R.J. Ewen, N. Guernion and N.M. Ratcliffe, Sensor. Actuat. B. 87 (2002) 207.
7. K. Zakrzewska, Thin Solid Films. 391 (2001) 229.
8. W. Cuna, Z. Jincai, W. Xinming, M. Bixian, S. Guoying, P. Pingan and F. Jiamo, Appl. Catal. B-Environ. 39 (2002) 269.
9. J. Bandara, K. Tennakone and P.P.B. Jayatilaka, Chemosphere. 49 (2002) 439.
10. Z. Wen, G. Wang, W. Lu, Q. Wang, Q. Zhang and J. Li, Cryst. Growth. Des. 7 (2007) 1722.
11. W. W. Wang, Y. J. Zhu and L. X. Yang, Adv. Funct. Mater. 17 (2007) 59.
12. A. Masuda, K. Imamori and H. Matsumura, Thin Solid Films. 411 (2002) 166.
13. J. Shang, W. Yao, Y. Zhua and N. Wu, Applied Appl. Catal. A-Gen. 257 (2004) 25.
14. F. Pourfayaz, A. Khodadadi, Y. Mortazavi and S.S. Mohajerzadeh, Sensor. Actuat. B. 108 (2005) 172.
15. Y. Chen, J. Zhu, X. Zhu, G. Ma, Z. Liu and N. Min, Mat. Sci. Eng. B. 99 (2003) 52.
16. F.M. Filho, A.Z. Simões, A. Ries, I.P. Silva, L. Perazolli, E. Longob and J.A. Varela, Ceramics Ceram. Int. 30 (2004) 2277.
17. S. Sun, G. Meng, G. Zhang and L. Zhang, Cryst. Growth. Des. 7 (2007) 1988.
18. M. M. Bagheri-Mohagheghi and M. Shokooh-Saremi, Thin Solid Films. 441 (2003) 238.
19. J.C. Jiang, K. Lian, E. I. Meletis, Thin Solid Films. 411 (2002) 203.
20. B. N. Mukashev, S.Zh. Tokmoldin, N.B. Beisenkhanov, S.M. Kikkarin, I.V. Valitova, V.B. Glazman, A.B. Aimagambetov, E.A. Dmitrieva and B.M. Veremenithev, Mat. Sci. Eng. B. 118 (2005) 164.
21. N. Lorrain, L. Chaffron, C. Carry, P. Delcroix and G. L. Caër, Mat. Sci. Eng. A, 367 (2004) 1.
22. F.I. Pires, E. Joanni, R. Savu, M.A. Zaghete, E. Longo and J.A. Varela, Mater. Lett. 62 (2008) 239.
23. D. S. Wu, C. Y. Han, S. Y. Wang, N. L. Wu and I. A. Rusakova, Mater. Lett. 53 (2002) 155.
24. Z. j. Jia, L. p. Zhu, G. H. Liao, Y. Yu and Y. W. Tang, Solid State Commun. 132 (2004) 79.
25. T. Kobayashi, Y. Kimura, H. Suzuki, T. Sato, T. Tanigaki, Y. Saito and C. Kaito, J. Cryst. Growth. 243 (2002) 143.
26. J. Chouvin, C. Branci, J. Sarradin, J. O. Fourcade, J. C. Jumas, B. Simon and Ph. Biensan, J. Power Sources. 81-82 (1999) 277.
27. B.D. Cullity, Elements of X-ray diffraction, Addison-Wesley Company, USA, 1978.
28. A. Esmaelzadeh Kandjani, M. Farzalipour Tabriz and B. Pourabbas, Mater. Res. Bull. 43 (2008) 645.
29. C. Wu, X. Qiao, J. Chen, H. Wang, F. Tan and S. Li, Mater. Lett. 60 (2006) 1828.